Journal of
Computational and Theoretical Nanoscience
Vol. 7, 1–7, 2010

Stress Distribution on a Single-Walled Carbon Nanohorn Embedded in an Epoxy Matrix Nanocomposite Under Axial Force

K. Momeni* and R. S. Yassar

Department of Mechanical Engineering-Engineering Mechanics, Michigan Technological University, Houghton, MI 49931, US

Carbon Nanotubes (CNTs) have been a subject of interest for most of the researches after their discovery, due to their superior mechanical properties and ability to be used as the reinforcement phase in nanocomposites. The other carbon structure which was discovered a few years after the discovery of CNTs was Carbon Nanohorns (CNHs). The structure of CNH is cone-shaped compared to the cylindrical shape of CNT's structure. This cone-shaped structure causes difficulties in finding the stress distribution in CNHs when embedded in the matrix phase of nanocomposites. In this paper the governing differential equation of the stress distribution on the CNHs placed in a nanocomposite matrix is derived using some simplifying assumptions. It has been shown here that while the stress distribution is symmetric for the special case of CNT, it is non-symmetric for the general CNHs and the maximum stress shifts toward the tip of CNH.

Keywords: Analytical Modeling, Nano-Structures, Stress Transfer, Carbon Nanohorn.

RESEARCH ARTICLE

1. INTRODUCTION

Few years after the discovery of CNTs by Iijima et al.[1] in 1991, CNHs were introduced by Harris et al. in 1994.[2] CNTs show unique mechanical properties, such as large elastic modulus which can reach up to 5 TPa[3–8] compared with elastic modulus of carbon fibers which is from 0.1 to 0.8 TP[9] and strength up to 63 GPa.[10] Discovery of CNTs made a great deal of interest among the scientists to explore new devices and applications. On the other hand, carbon nanohorns have a high strength sp^2 carbon-carbon bond, and they can be produced with purity higher than 90%. This is because CNHs don't need the use of catalytic particles for synthesis in contrast to CNTs.[11,12] In addition the surface area of the carbon nanohorns is 300 to 400 m^2/g compared to 178 m^2/g for the multi-walled CNTs and 285 m^2/g for single-walled CNTs. Furthermore, surface area of CNHs can be improved by a post treatment process up to more than 1000 m^2/g.[13–17]

Due to the above advantages, it is expected that CNH reinforced nanocomposites have a higher mechanical properties than the CNT reinforced nanocomposites. In this paper the differential equations governing the distribution of stress on a carbon nanohorn which is placed in an epoxy matrix under axial loading will be investigated using Cox model[18] and it will be compared with the stress distribution model of the CNTs.[19]

2. PROBLEM DEFINITION

The representative volume element (RVE) for this problem is shown in Figure 1 and the side views of the CNH in the RVE are shown in Figure 2. We assumed that $2L$ is the longitudinal length of the RVE. In addition $2L_f$ represents the longitudinal length of the embedded CNH. We have considered $2L$ and $2L_f$ instead of simply considering L and L_f because in the case of zero cone angle, i.e., a cylindrical tube like CNT, the stress is symmetric about the middle plane.

The outer radius of the CNH is $r_o = a + z \cdot \tan(\alpha)$; where a represents the CNH's outer diameter at $z = 0$. Considering the CNH's thickness as t then the relation between the outer and inner radius of the CNH would be $r_i = r_o - t$.

The equilibrium equations in absence of body forces, for axisymmetric problem in terms of cylindrical coordinate (r, θ, z) are:[20]

$$\frac{\partial \sigma_{rr}}{\partial r} + \frac{\partial \tau_{rz}}{\partial z} + \frac{\sigma_{rr} - \sigma_{\theta\theta}}{r} = 0 \qquad (1a)$$

*Author to whom correspondence should be addressed.

 1546-1955/2010/7/001/007 doi:10.1166/jctn.2010.1450

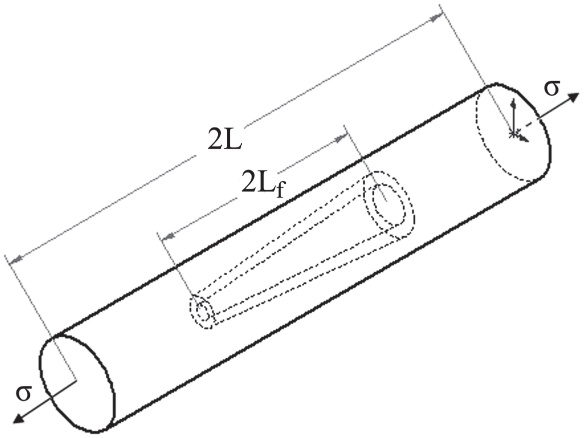

Fig. 1. RVE of a CNH with length of $2L_f$ embedded in a matrix with length of 2L. The composite is then being subjected to the overall stress of σ along the cylindrical axis.

$$\frac{\partial \tau_{rz}}{\partial r}+\frac{\partial \sigma_{zz}}{\partial z}+\frac{\tau_{rz}}{r}=0 \tag{1b}$$

Assuming the u and w as displacement along r and z direction, the geometrical equations for CNH can be written as:

$$\varepsilon_{rr}=\frac{\partial u}{\partial r} \tag{2a}$$

$$\varepsilon_{\theta\theta}=\frac{u}{r} \tag{2b}$$

$$\varepsilon_{zz}=\frac{\partial w}{\partial z} \tag{2c}$$

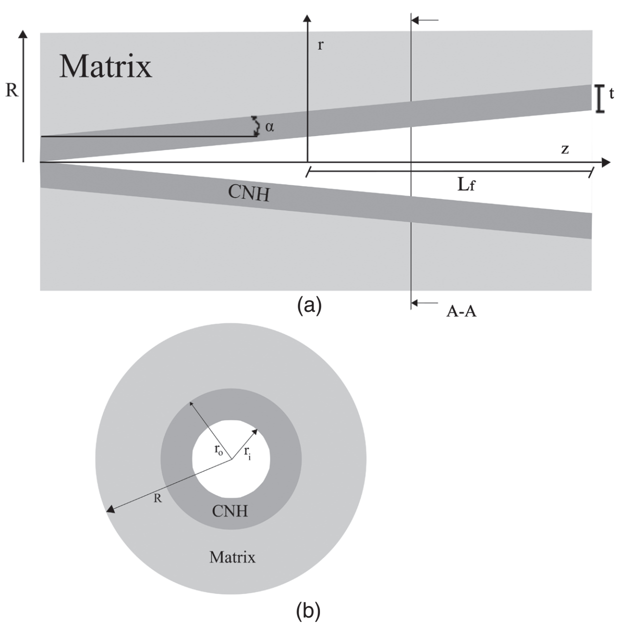

Fig. 2. (a) Side view and (b) cross-sectional view, A-A, of the RVE shown in Figure 1. The inner and outer radiuses, r_i and r_0, of CNH change along the z-axis as a function of cone angle, 2α, while its thickness, t, remains constant.

$$\gamma_{rz}=\frac{\partial u}{\partial z}+\frac{\partial w}{\partial r} \tag{2d}$$

Assuming CNH and matrix as elastic materials, the constitutive equations are:

$$\varepsilon_{rr}=\frac{1}{E}[\sigma_{rr}-\nu(\sigma_{\theta\theta}+\sigma_{zz})] \tag{3a}$$

$$\varepsilon_{\theta\theta}=\frac{1}{E}[\sigma_{\theta\theta}-\nu(\sigma_{zz}+\sigma_{rr})] \tag{3b}$$

$$\varepsilon_{zz}=\frac{1}{E}[\sigma_{zz}-\nu(\sigma_{rr}+\sigma_{\theta\theta})] \tag{3c}$$

$$\gamma_{rz}=\frac{\tau_{rz}}{G} \tag{3d}$$

The other strain components are vanished due to the problem configuration and geometry of applied forces, i.e., axial loading.

In the next step we will define the boundary equations for the above mentioned governing equations. The boundary conditions (4) are describing the force balance at the boundaries of the RVE. The Eq. (5) are due to the force balance at the CNH-matrix interface. According to the type of loading, there is no traction along radial direction on surface of the RVE, i.e., Eq. (4a). The stress σ is applied on the extremes of the CNH along its axis of symmetry, which leads to Eq. (4b). In Eq. (4b) $\hat{e}_z$ is the unit vector along the z-axis.

$$\begin{cases} T^m|_{r=R}=0 & (4a)\\ T^m|_{z=\pm L_f}=\pm\sigma\cdot\hat{e}_z & (4b)\end{cases}$$

The force balance between the CNH and matrix along the radial direction and at the extreme ends, lead to Eqs. (5a, b).

$$\begin{cases} T^f|_{-L_f<z<L_f,\, r=r_o(z)}=T^m|_{-L_f<z<L_f,\, r=r_o(z)} & (5a)\\ T^f|_{z=\pm L_f,\, r_i<r<r_o}=T^m|_{z=\pm L_f,\, r_i<r<r_o} & (5b)\end{cases}$$

3. SOLUTION

In general, the integration of Eq. (1b) with respect to r from r_i to r_o for a reinforcing CNH designated by superscript f:

$$\frac{1}{\pi(r_o^2-r_i^2)}\int_{r_i}^{r_o}\frac{\partial\sigma_{zz}^f}{\partial z}(2\pi r)\,dr + \frac{1}{\pi(r_o^2-r_i^2)}\int_{r_i}^{r_o}\frac{1}{r}\frac{\partial}{\partial r}(r\tau_{rz}^f)(2\pi r)\,dr=0 \tag{6}$$

where the first part of (6) can be defined as an average axial normal stress over the cross section of the CNH as below:

$$\bar{\sigma}_{zz}^f=\frac{1}{\pi(r_o^2-r_i^2)}\int_{r_i}^{r_o}\sigma_{zz}^f(r,z)\cdot(2\pi r)\,dr \tag{7}$$

Differentiation of (7) with respect to z and using (6) leads to:

$$\frac{d\bar{\sigma}^f_{zz}}{dz} = \frac{1}{\pi(r_o^2 - r_i^2)}\Bigg[-\frac{2\cdot tg(\alpha)}{r_o - r_i}\int_{r_i}^{r_o}\sigma^f_{zz}(r,z)(2\pi\cdot r)\cdot dr + tg(\alpha)(2\pi\cdot r_o)\sigma^f_{zz}(r_o,z) - tg(\alpha)(2\pi\cdot r_i)\sigma^f_{zz}(r_i,z) - 2\pi(r_o\tau^f_o - r_i\tau^f_i)\Bigg] \quad (8)$$

By assuming that:

$$\frac{\partial\sigma^f_{zz}}{\partial z} = f(z) \quad (9)$$

and using (1b) we have:

$$\frac{\partial\tau^f_{rz}}{\partial r} + f(z) + \frac{\tau^f_{rz}}{r} = 0 \quad (10)$$

This is a first order linear differential equation in terms of τ^f_{rz} which its solution leads to:

$$\tau^f_{rz} = -\frac{1}{2}f(z)\cdot r + \frac{c_1}{r} \quad (11)$$

Assuming $\tau^f_{rz}|_{r=r_i} = 0$ which means no matrix penetration into the hollow part of the CNH we have:

$$\tau^f_{rz} = \frac{1}{2}f(z)\cdot r\left[\frac{r_i^2}{r^2} - 1\right] \quad (12)$$

Using (11) and (12) we have:

$$c_1 = \frac{1}{2}f(z)\cdot r_i^2 \quad (13)$$

For simplicity we will represent $\tau^f_{rz}|_{r=r_o}$ by τ^f_o; So we obtain:

$$f(z) = \frac{2}{r_o}\left[\frac{r_o^2}{r_i^2 - r_o^2}\right]\tau^f_o = \frac{2r_o}{r_i^2 - r_o^2}\tau^f_o(z) \quad (14a)$$

$$\tau^f_{rz} = \frac{r_o\cdot r}{r_i^2 - r_o^2}\left[\frac{r_i^2}{r^2} - 1\right]\tau^f_o(z) \quad (14b)$$

The boundary condition of (4a) implies that there is no radial normal stress and shear stress on the circumference of the matrix. So we may rewrite Eq. (4a) as:

$$\sigma^m_{rr}|_{r=R} = 0 \quad (15a)$$

$$\tau^m_{zr}|_{r=R} = 0 \quad (15b)$$

In a similar manner rewriting Eq. (5a) leads to:

$$\sigma^f_{rr}|_{-L_f<z<L_f,\, r=r_o} = \sigma^m_{rr}|_{-L_f<z<L_f,\, r=r_o} \quad (16a)$$

$$\tau^f_{zr}|_{-L_f<z<L_f,\, r=r_o} = \tau^m_{zr}|_{-L_f<z<L_f,\, r=r_o} \quad (16b)$$

Now integrating (1b) with respect to r from r_o to R and using (15b) leads to,

$$\frac{1}{\pi(R^2 - r_o^2)}\int_{r_o}^{R}\frac{\partial\sigma^m_{zz}}{\partial z}(2\pi r)\cdot dr + \frac{1}{\pi(R^2 - r_o^2)}\int_{r_o}^{R}\frac{1}{r}\frac{\partial}{\partial r}(r\tau^m_{rz})(2\pi r)\cdot dr = 0 \quad (17)$$

Considering,

$$\bar{\sigma}^m_{zz}(z) = \frac{1}{\pi(R^2 - r_o^2)}\int_{r_o}^{R}\sigma^m_{zz}(r,z)\cdot(2\pi r)\cdot dr \quad (18)$$

then by assuming,

$$\frac{\partial\bar{\sigma}^m_{zz}}{\partial z} = g(z) \quad (19)$$

were g(z) is an unknown function that must be determined. Inserting (19) in (17) and integrating with respect to r form r to R leads to:

$$\frac{1}{\pi(R^2 - r^2)}\int_{r}^{R}g(z)\cdot(2\pi r)\,dr + \frac{1}{\pi(R^2 - r^2)}\int_{r}^{R}\frac{1}{r}\cdot\frac{\partial}{\partial r}(r\tau^m_{rz})\cdot(2\pi r)\,dr = 0$$
$$\Rightarrow\ g(z) = \frac{2}{R^2 - r^2}r\cdot\tau^m_{rz}(r)$$
$$\Rightarrow\ \tau^m_{rz} = \frac{g(z)}{2}\cdot\frac{R^2 - r^2}{r} \quad (20)$$

Using (20) and (5b),

$$g(z) = \frac{2\cdot r_o}{R^2 - r_o^2}\tau^f_o \quad (21)$$

Substituting (21) in (20),

$$\tau^m_{rz}(r) = \frac{r_o}{R^2 - r_o^2}\left(\frac{R^2 - r^2}{r}\right)\cdot\tau^f_o \quad (22)$$

and assuming that$|\partial u/\partial z| \prec\prec |\partial w/\partial r|$, i.e., the radial displacement along the radii is much smaller than the axial displacement along the radii, and (2d) and (3d),

$$\tau^f_{rz} = G^f\frac{\partial w^f}{\partial r} \quad (23a)$$

$$\tau^m_{rz} = G^m\frac{\partial w^m}{\partial r} \quad (23b)$$

Using (23b) and (22) we have,

$$\tau^f_o = G^m\frac{R^2 - r_o^2}{R^2 - r^2}\cdot\frac{r}{r_o}\cdot\frac{\partial w^m}{\partial r} \quad (24)$$

Rearranging (24) and integrating from r_o to R leads to,

$$\tau^f_o\int_{r_o}^{R}\left(\frac{R^2}{r} - r\right)dr = \int_{r_o}^{R}G^m\frac{(R^2 - r_o^2)}{r_o}dw^m$$
$$\Rightarrow\ \tau^f_o = G^m\frac{R^2 - r_o^2}{r_o}\frac{w^m_R - w^m_{r_o}}{R^2\ln(R/r_o) - 1/2(R^2 - r_o^2)} \quad (25)$$

RESEARCH ARTICLE

Substitution of (25) into (22) results in,

$$\tau_{rz}^m(r) = G^m \frac{R^2-r^2}{r}\left[\frac{w_R^m - w_{r_o}^m}{R^2\ln(R/r_o) - 1/2(R^2-r_o^2)}\right] \quad (26)$$

Putting (26) into (23b) leads to:

$$\frac{\partial w^m}{\partial r} = \frac{R^2-r^2}{r}\left[\frac{w_R^m - w_{r_o}^m}{R^2\ln(R/r_o)-1/2(R^2-r_o^2)}\right] \xrightarrow{\int_{r_o}^r}$$

$$w_r^m(r,z) = w_{r_o}^m + \left[\frac{(w_R^m - w_{r_o}^m)\cdot(R^2\ln(r/r_o)-1/2(r^2-r_o^2))}{R^2\ln(R/r_o)-1/2(R^2-r_o^2)}\right] \quad (27)$$

Assuming $\sigma_{\theta\theta}+\sigma_{\gamma\gamma} \ll \sigma_{zz}$ for both matrix and the CNH, due to the fact that we considered the nanocomposite under axial loading, and using (2c), (3c) and noting that $r(z) = r_o(z)+g$, then we have:

$$\sigma_{zz}^f = E^f\frac{\partial w^f}{\partial z}, \qquad \sigma_{zz}^m = E^m\frac{\partial w^m}{\partial z} \quad (28)$$

$$\begin{aligned}\sigma_{zz}^m = {} & \sigma_{zz}^m|_{r=r_o} + \left(R^2\ln(r/r_o) - \frac{1}{2}(r^2-r_o^2)\right) \\ & \cdot\left(R^2\ln(R/r_o)-\frac{1}{2}(R^2-r_o^2)\right)^{-1}\cdot[\sigma_{zz}^m|_{r=R}-\sigma_{zz}^m|_{r=r_o}] \\ & +(w_R^m - w_{r_o}^m)\cdot E^m\cdot tg(\alpha) \\ & \cdot\left[\left(R^2\frac{r_o}{r}\left(\frac{1}{r}-\frac{r}{r_o^2}\right)-(r-r_o)\right)\right. \\ & \cdot\left(R^2\ln\left(\frac{R}{r_o}\right)-\frac{1}{2}(R^2-r_o^2)\right)^{-1} \\ & -\left[R^2\ln\left(\frac{r}{r_o}\right)-\frac{1}{2}(r^2-r_o^2)\right]\cdot\left[-\frac{R^2}{r_o}+r_o\right] \\ & \left.\cdot\left[R^2\ln\left(\frac{R}{r_o}\right)-\frac{1}{2}(R^2-r_o^2)\right]^{-2}\right]\end{aligned} \quad (29)$$

Considering the force balance of the composite along the z axis:

$$\pi R^2\sigma = \int_{r_i}^{r_o}\sigma_{zz}^f\cdot(2\pi r)\,dr + \int_{r_o}^{R}\sigma_{zz}^m(2\pi r)\,dr \quad (30)$$

Using (7), (29) and (30) we have:

$$\begin{aligned}& \sigma_{zz}^m|_{r=R}-\sigma_{zz}^m|_{r=r_o} \\ & = \left(R^2\ln(R/r_o)-\frac{1}{2}(R^2-r_o^2)\right) \\ & \quad\cdot\left(R^4\ln(R/r_o)-\frac{1}{4}(R^2-r_o^2)\cdot(3R^2-r_o^2)\right)^{-1} \\ & \quad\cdot(R^2\sigma-\bar{\sigma}_{zz}^f(r_o^2-r_i^2)-\sigma_{zz}^m|_{r=r_o}(R^2-r_o^2)) \\ & \quad-(2\cdot E_m.tg(\alpha)\cdot(w_R^m-w_{r_o}^m)) \\ & \quad\cdot\left(R^4\ln(R/r_o)-\frac{1}{4}(R^2-r_o^2)\cdot(3R^2-r_o^2)\right)^{-1} \\ & \quad\cdot\left[R^2\cdot r_o\cdot\ln\left(\frac{R}{r_o}\right)-\frac{R^2}{2r_o}(R^2-r_o^2)\right. \\ & \quad-\frac{1}{3}(R^3-r_o^3)+\frac{r_o}{2}(R^2-r_o^2)-\left(r_o-\frac{R^2}{r_o}\right) \\ & \quad\cdot\left(R^2\ln\left(\frac{R}{r_o}\right)-\frac{1}{2}(R^2-r_o^2)\right)^{-1} \\ & \quad\left.\cdot\left(\frac{R^2}{2}r_o^2-\frac{1}{8}r_o^4+\frac{1}{2}R^4\ln\left(\frac{R}{r_o}\right)-\frac{3}{4}R^4\right)\right]\end{aligned} \quad (31)$$

From (8) and assuming no matrix penetration inside the CNH, then:

$$\begin{aligned}\frac{d\bar{\sigma}_{zz}^f}{dz} = {} & 2\cdot tg(\alpha)\cdot(r_o\sigma_{zz}^f(r_o,z)-r_i\sigma_{zz}^f(r_i,z)-(r_o-r_i)\bar{\sigma}_{zz}^f) \\ & \cdot(r_o^2-r_i^2)^{-1}-\frac{2r_o}{r_o^2-r_i^2}\tau_o^f\end{aligned} \quad (32)$$

From (26), (29b), (31), and (32) it follows that,

$$\begin{aligned}\frac{d^2\bar{\sigma}_{zz}^f}{dz^2} = {} & \frac{2tg^2(\alpha)}{(r_o^2-r_i^2)}\left[\sigma_{zz}^f(r_o,z)-\sigma_{zz}^f(r_i,z)-\frac{2}{r_o+r_i}\right. \\ & \left.\times(r_o\sigma_{zz}^f(r_o,z)-r_i\sigma_{zz}^f(r_i,z)-(r_o-r_i)\bar{\sigma}_{zz}^f)\right] \\ & +\frac{2\tan(\alpha)}{(r_o^2-r_i^2)}\left[r_o\cdot\left.\frac{\partial\sigma_{zz}^f}{\partial z}\right|_{r=r_o}-r_i\cdot\left.\frac{\partial\sigma_{zz}^f}{\partial z}\right|_{r=r_i}-(r_o-r_i)\frac{\partial\bar{\sigma}_{zz}^f}{\partial z}\right] \\ & -\frac{2G_m}{E_m}\frac{R^2-r_o^2}{r_o^2-r_i^2}(R^2\sigma+(r_o^2-R^2).\sigma_{zz}^m|_{r=r_o}+(r_i^2-r_o^2)\bar{\sigma}_{zz}^f) \\ & \cdot\left(R^4\ln\left(\frac{R}{r_o}\right)-\frac{1}{4}(3R^2-r_o^2)(R^2-r_o^2)\right)^{-1} \\ & +2(w_R^m-w_{r_o}^m)\cdot\left(R^2\ln\left(\frac{R}{r_o}\right)-\frac{1}{2}(R^2-r_o^2)\right)^{-1} \\ & \cdot\left\{\frac{G_m\cdot\tan(\alpha)}{r_o}\times\left[\frac{1}{r_o^2-r_i^2}\left(R^2+r_o^2-(R^2-r_o^2)^2\right.\right.\right. \\ & \left.\left.\cdot\left(R^2\ln\left(\frac{R}{r_o}\right)-\frac{1}{2}(R^2-r_o^2)\right)^{-1}\right)+\frac{R^2-r_o^2}{(r_o+r_i)^2}\right] \\ & +2G_m\tan(\alpha) \\ & \cdot\left(R^4\ln\left(\frac{R}{r_o}\right)-\frac{1}{4}(3R^2-r_o^2)(R^2-r_o^2)\right)^{-1} \\ & \cdot\frac{R^2-r_o^2}{r_o^2-r_i^2}\times\left[R^2r_o\ln\left(\frac{R}{r_o}\right)-\frac{R^2}{2r_o}(R^2-r_o^2)\right. \\ & -\frac{R^3-r_o^3}{3}+\frac{r_o}{2}(R^2-r_o^2)-(r_o^2-R^2)^{-1} \\ & \cdot\left(r_o\left(R^2\ln\left(\frac{R}{r_o}\right)-\frac{1}{2}(R^2-r_o^2)\right)\right)^{-1} \\ & \left.\left.\cdot\left(\frac{R_2r_o^2}{2}-\frac{r_o^4}{8}+\frac{R^4}{2}\ln\left(\frac{R}{r_o}\right)-\frac{3}{8}R^4\right)\right]\right\}\end{aligned} \quad (33)$$

RESEARCH ARTICLE

Due to (8) and no matrix penetration inside the CNH (i.e., $\tau_i^f = 0$) and $\bar{\sigma}_{zz}^f = \bar{\sigma}_{zz}^f(z)$ the following equation can be obtained:

$$\frac{d\bar{\sigma}_{zz}^f}{dz} = -2\frac{r_o \cdot \tau_o^f}{r_o^2 - r_i^2} \tag{34}$$

Inserting (25) in (38) we have:

$$\frac{w_R^m - w_{r_o}^m}{R^2 \ln(R/r_o) - \frac{1}{2}(R^2 - r_o^2)} = -\frac{r_o^2 - r_i^2}{2G_m(R^2 - r_o^2)}\frac{d\bar{\sigma}_{zz}^f}{dz} \tag{35}$$

Assuming that the bounding between the CNH and matrix to be perfect, i.e., no sliding occurs at the CNH-Matrix interface, we have:

$$\varepsilon_{zz}^m|_{r=r_o} = \varepsilon_{zz}^f|_{r=r_o} \;\Rightarrow\; \sigma_z^m|_{r=r_o} = \frac{E^m}{E^f}\sigma_{zz}^f|_{r=r_o} \tag{36}$$

Assuming low volume fraction of the CNH,

$$\sigma_{zz}^f \approx \bar{\sigma}_{zz}^f \tag{37}$$

and using (33), (35), (36), and (37) we have:

$$\frac{d^2\bar{\sigma}_{zz}^f}{dz^2} + \Phi(z)\frac{d\bar{\sigma}_{zz}^f}{dz} + \Gamma(z)\bar{\sigma}_{zz}^f = \Xi(z) \tag{39}$$

where Φ(z), Γ(z), and Ξ(z) have been defined in (40a–c). σ in (40c) is the applied axial stress to the RVE, which is constant. Differential Eq. (39) is a second order linear one which its coefficients are functions of independent variable, z. Therefore it can be solved using power series method.

$$\begin{aligned}\Phi(z) = {} & \frac{1}{G^m}\frac{r_o^2 - r_i^2}{R^2 - r_o^2} \\ & \times\Bigg\{\frac{G_m \cdot \tan(\alpha)}{r_o} \times \Bigg[\frac{1}{r_o^2 - r_i^2}\Bigg(R^2 + r_o^2 - (R^2 - r_o^2)^2 \\ & \cdot\left(R^2\ln\left(\frac{R}{r_o}\right) - \frac{1}{2}(R^2 - r_o^2)\right)^{-1}\Bigg) + \frac{R^2 - r_o^2}{(r_o + r_i)^2}\Bigg] \\ & + 2G_m\tan(\alpha)\cdot\Bigg(R^4\ln\left(\frac{R}{r_o}\right) \\ & - \frac{1}{4}(3R^2 - r_o^2)(R^2 - r_o^2)\Bigg)^{-1}\frac{R^2 - r_o^2}{r_o^2 - r_i^2} \\ & \times\Bigg[R^2 r_o\ln\left(\frac{R}{r_o}\right) - \frac{R^2}{2r_o}(R^2 - r_o^2) \\ & - \frac{R^3 - r_o^3}{3} + \frac{r_o}{2}(R^2 - r_o^2) \\ & - \frac{r_o^2 - R^2}{r_o(R^2\ln(R/r_o) - 1/2(R^2 - r_o^2))} \\ & \cdot\left(\frac{R_2 r_o^2}{2} - \frac{r_o^4}{8} + \frac{R^4}{2}\ln\left(\frac{R}{r_o}\right) - \frac{3}{8}R^4\right)\Bigg]\Bigg\}\end{aligned} \tag{40a}$$

$$\begin{aligned}\Gamma(z) = {} & -\frac{R^2 - r_o^2}{r_o^2 - r_i^2}\frac{1}{1+\nu^m}\left[(r_o^2 - r_i^2) + \frac{E^m}{E^f}(R^2 - r_o^2)\right] \\ & \cdot\left[R^4\ln\left(\frac{R}{r_o}\right) - \frac{1}{4}(3R^2 - r_o^2)(R^2 - r_o^2)\right]^{-1}\end{aligned} \tag{40b}$$

$$\begin{aligned}\Xi(z) = {} & -\frac{R^2 - r_o^2}{r_o^2 - r_i^2}\frac{1}{1+\nu^m}(R^2\sigma) \\ & \cdot\left(R^4\ln\left(\frac{R}{r_o}\right) - \frac{1}{4}(3R^2 - r_0^2)(R^2 - r_o^2)\right)^{-1}\end{aligned} \tag{40c}$$

Equation (39) is completely consistent with the previous works on CNTs[21] and CNHs.[22]

4. RESULTS AND DISCUSSION

Here the differential Eq. (39) has been solved numerically for the case of epoxy matrix and CNH while six different cone angles have been considered. Here we have used the mechanical properties of CNT, due to the lack of data for the mechanical properties of CNH. It is justified because both CNT and CNH have the same inter atomic bonding, i.e., sp^2. Therefore, it is expected that the mechanical properties of the CNH would not be much different from the mechanical properties of CNT. The properties of these materials are considered as follows; $\alpha = 20°$, $10°$, $5°$, $2°$, $1°$, and $0°$, $E_m = 2.41$ GPa, $E_f = 1000$ GPa, $\nu_m = 0.25$, $a = 0.8$ nm, $t = 0.34$ nm, $G_m = E_m/2(1+\nu_m)$, $\sigma = 1$ GPa, L_f =100 nm and $R > 5 \times \max(r_o) = 250$ nm.[23–24] For solving this problem Maple 9.5[25] has been used. This problem has been solved with Runge-Kutta-Fehlberg[26] method which results in a fifth order accurate solution. The CNH's mean stress distribution versus the distance from its tip has been plotted along its longitudinal axis of symmetry in Figure 3. For solving this problem we need two boundary conditions; Therefore we used the value of mean fiber stress at $z = 0$ and $z = L_f$ for the case of open-ended CNTs.[21]

As it has been shown in Figure 3, the stress distribution along the CNH is a non-linear function of the cone angle. Moreover the maximum mean normal stress does not occur at the middle of the CNH as it does in the case of open-ended CNTs[21] and conventional rod-shape fibers.[27] From Figure 3 we can conclude that the larger the cone angle, the further the deviation of location of maximum mean stress from the middle of the fiber.

In the case of zero cone angle, the maximum occurs at the middle of the fiber which is plausible due to the fact that in this case the governing differential equations would be exactly the same as the case of hollow cylindrical fiber.[21]

In addition to the deviation of maximum mean normal stress, the rate of change of mean stress is not symmetric in the case of CNH. If we classify the stress distribution on the CNH into two sections, one from the CNH's tip to max value of stress and the other from the max value of stress to the opposite end of CNH, it can be seen that the rate of change of mean stress is higher at the first section compared to the other section (Fig. 4). Furthermore the

RESEARCH ARTICLE

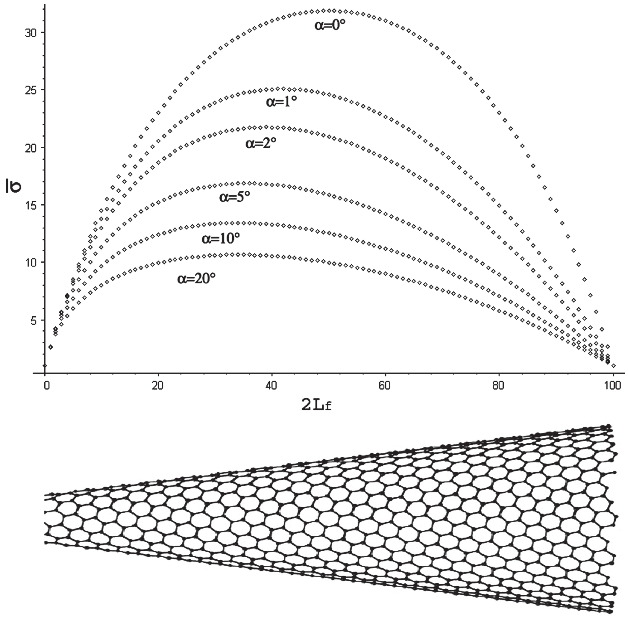

Fig. 3. Mean stress, $\bar{\sigma}$, versus CNH distance along the axes of CNH, $2L_f$. While the maximum stress occurs at the middle for the CNT, for the case of CNH, the position of maximum stress moves toward the tip of CNH.

rate of change of maximum mean stress is lower at the higher angles but it will change abruptly at the smaller angles. These features happen due to the fact that the stress transfers to the CNH due to the shear stress between the matrix and CNH. The amount of transferred stress at the extreme ends of the CNH is negligible and it rises to a maximum somewhere in between. On the other hand, the cross-section area of the CNH changes from a minimum value to a maximum one. While the stress is proportional to the amount of transferred shear stress, it is inversely proportional to the cross-section area. It is expected that the derived mathematical framework provides a computational

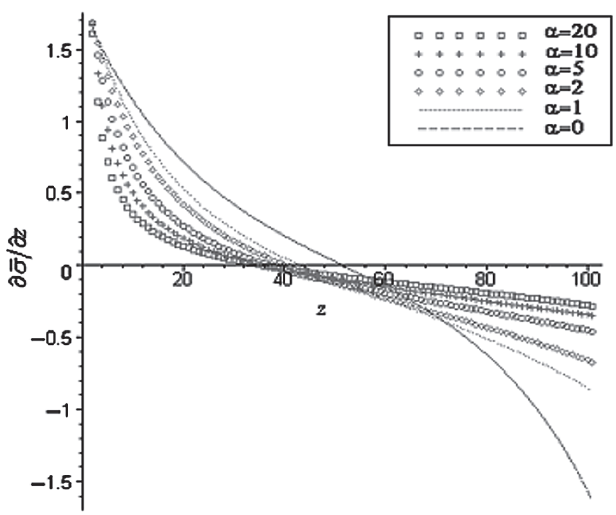

Fig. 4. Rate of change of mean stress along the CNH, i.e., $\partial\bar{\sigma}/\partial z$.

means for future design of new generation of nanocomposites reinforced with CNHs.

5. CONCLUSION

The superior properties of the CNHs compared to CNTs, such as higher purity and surface areas, promise an increasing application of CNHs in future nanocomposites. In this work a rigorous mathematical framework to model the stress distribution at the interface of a CNH and composite matrix is derived. It has been shown that the stress distribution along the CNH is a non-linear function of the cone angle. Also we showed that the larger the cone angle, the bigger is the deviation of mean stress distribution from the symmetric case. Although the formula obtained in this paper are for the case of CNHs but it is also applicable to the CNTs because CNTs are special case of CNHs with zero cone angle.

NOMENCLATURE

z Axial coordinate of the RVE[a]
r Radial coordinate of the RVE
R Radius of the RVE
α Half cone angle of the CNH[b]
r_o Outer radius of the CNH
r_i Inner radius of the CNH
a CNH's outer diameter at $z = 0$
t Thickness of CNH's wall
ε Strain
σ Constant applied axial stress to the RVE
$\bar{\sigma}$ Average axial normal stress
τ Shear Stress
ν Poisson's ratio
G Shear Modulus
γ Shear strain
m Parameters associated to matrix material
f Parameters associated to CNH
u Radial displacement
w Axial displacement
T Traction
L Length of the RVE

[a]Representative Volume Element.
[b]Carbon Nano Horn.

Acknowledgments: We appreciate Ms. Soghrati for the help and the Michigan Technological University for providing the financial support.

References

1. S. Iijima, *Nature* 56, 354 **(1991)**.
2. P. J. F. Harris, M. L. H. Green, and S. C. Tsang, *J. Chem. Soc.-Faraday Trans.* 89, 2799 **(1994)**.
3. E. W. Wong, P. E. Sheehan, and C. M. Lieber, *Science* 277, 1971 **(1997)**.

4. O. Lourie, H. D. Wagner, *J. Mat. Res.* 13, 2418 (**1998**).
5. G. Overney, W. Zhong, and D. Tomanek, *Zeitschrift Fur Physik D-Atoms Molecules and Clusters* 27, 93 (**1993**).
6. J. P. Lu, *Physical Rev. Lett.* 79, 1297 (**1997**).
7. M. M. Treacy, T. W. Ebessen, and J. M. Gibson, *Nature* 381, 678 (**1996**).
8. P. Zhang, Y. Huang, P. H. Geubelle, P. A. Klein, and K. C. Hwang, *International Journal of Solids and Structures* 39, 3893 (**2002**).
9. P. Morgan, Carbon Fibers and Their Composites, CRC Press (**2005**) p. 811.
10. M. Yu, O. Lourie, M. J. Dyer, T. F. Kelly, and R. S. Ruoff, *Science* 287, 637 (**2000**).
11. S. Iijima, M. Yudasaka, R. Yamada, S. Bandow, K. Suenaga, F. Kokai, K. Takahashi, *Chem. Phys. Lett.* 309, 165 (**1999**).
12. D. Kasuya, M. Yudasaka, K. Takahashi, F. Kokai, and S. Iijima, *J. Phys. Chem. B.* 106, 4947 (**2002**).
13. K. Murata, K. Kaneko, W. A. Steele, F. Kokai, T. Takahashi, D. Kasuya, M. Yudusaka, and S. Iijima, *J. Phys. Chem. B* 105, 10210 (**2001**).
14. S. Iijima, *Physica B-Condensed Matter* 323, 1 (**2002**).
15. S. Iijima, *Japan Nanonet Bulletin* 23 (**2004**).
16. S. Inoue, N. Ichikuni, T. Susuki, T. Uematsu, and K. Kaneko, *J. Phys. Chem. B*, 102, 4689 (**1998**).
17. Y. Ye, C. C. Ahn, C. Witham, B. Fults, J. Liu, G. RinzlerA, D. Colbert, K. A. Smith, and R. E. Smalley, *Appl. Phys. Lett.* 74, 2307 (**1999**).
18. H. L. Cox, *Br. J. Appl. Phys.* 3, 72 (**1952**).
19. K. Q. Xiao and L. C. Zhang, *J. Mat. Science* 39, 4481 (**2004**).
20. A. P. Boresi and K. P. Chong, Elasticity in Engineering Mechanics, 2nd edn., Wiley-Interscience (**2000**).
21. K. Momeni, A. Alasty, Stress distribution on open-ended carbon nanotubes, *MicroNano08*, Clear Water Bay, Kowloon, Hong Kong, June (**2008**).
22. K. Momeni, A. Alasty, and A. Shokuhfar, Governing differential equation of the stress distribution on a single walled carbon nanohorn embedded in an epoxy matrix nanocomposite, *NS2008, Second Conf. Nanostructures*, Kish Island, Iran, March (**2008**).
23. S. Namilae, N. Chandra, and C. Shet, . *Phys. Lett.* 387, 247 (**2004**).
24. J. R. Callister, Materials Science and Engineering an Introduction, 5th edn., John Willey (**2000**).
25. M. L. Abell and J. B. Braselton, Maple by Example, Elsevier Inc. (**2005**).
26. M. K. Jain, S. R. K. Iyengar, and R. K. Jain, Numerical Methods for Scientific and Engineering Computation, New Age International Publishers (**2003**).
27. X. L. Gao and K. Li, *International Journal of Solids and Structures* 42, 1649 (**2005**).

Received: 4 July 2009. Accepted: 3 September 2009.

RESEARCH ARTICLE